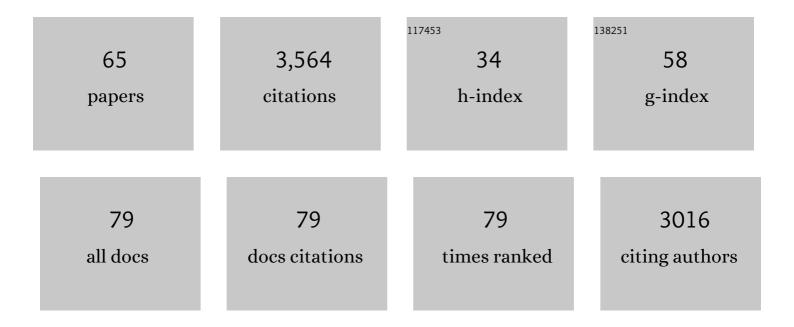
## Juan Carlos Afonso

List of Publications by Year in descending order

Source: https://exaly.com/author-pdf/2365088/publications.pdf Version: 2024-02-01



#	Article	IF	CITATIONS
1	The Composition and Evolution of Lithospheric Mantle: a Re-evaluation and its Tectonic Implications. Journal of Petrology, 2009, 50, 1185-1204.	1.1	540
2	Integrated geophysicalâ€petrological modeling of the lithosphere and sublithospheric upper mantle: Methodology and applications. Geochemistry, Geophysics, Geosystems, 2008, 9, .	1.0	200
3	Crustal and mantle strengths in continental lithosphere: is the jelly sandwich model obsolete?. Tectonophysics, 2004, 394, 221-232.	0.9	175
4	Mantle Recycling: Transition Zone Metamorphism of Tibetan Ophiolitic Peridotites and its Tectonic Implications. Journal of Petrology, 2016, 57, 655-684.	1.1	137
5	The structure and evolution of the lithosphere–asthenosphere boundary beneath the Atlantic–Mediterranean Transition Region. Lithos, 2010, 120, 74-95.	0.6	126
6	3â€Ð multiobservable probabilistic inversion for the compositional and thermal structure of the lithosphere and upper mantle. I: <i>a priori</i> petrological information and geophysical observables. Journal of Geophysical Research: Solid Earth, 2013, 118, 2586-2617.	1.4	121
7	LitMod3D: An interactive 3â€D software to model the thermal, compositional, density, seismological, and rheological structure of the lithosphere and sublithospheric upper mantle. Geochemistry, Geophysics, Geosystems, 2009, 10, .	1.0	107
8	Seismic evidence of on-going sublithosphere upper mantle convection for intra-plate volcanism in Northeast China. Earth and Planetary Science Letters, 2016, 433, 31-43.	1.8	107
9	Tibetan chromitites: Excavating the slab graveyard. Geology, 2015, 43, 179-182.	2.0	94
10	Long-term interaction between mid-ocean ridges and mantle plumes. Nature Geoscience, 2015, 8, 479-483.	5.4	92
11	Global Crustal Thickness and Velocity Structure From Geostatistical Analysis of Seismic Data. Journal of Geophysical Research: Solid Earth, 2019, 124, 1626-1652.	1.4	86
12	3â€Ð multiâ€observable probabilistic inversion for the compositional and thermal structure of the lithosphere and upper mantle. II: General methodology and resolution analysis. Journal of Geophysical Research: Solid Earth, 2013, 118, 1650-1676.	1.4	78
13	Density structure and buoyancy of the oceanic lithosphere revisited. Geophysical Research Letters, 2007, 34, .	1.5	77
14	Comprehensive plate models for the thermal evolution of oceanic lithosphere. Geochemistry, Geophysics, Geosystems, 2013, 14, 3751-3778.	1.0	73
15	A global reference model of the lithosphere and upper mantle from joint inversion and analysis of multiple data sets. Geophysical Journal International, 2019, 217, 1602-1628.	1.0	72
16	Thermal expansivity and elastic properties of the lithospheric mantle: results from mineral physics of composites. Physics of the Earth and Planetary Interiors, 2005, 149, 279-306.	0.7	71
17	On the Vp/Vs–Mg# correlation in mantle peridotites: Implications for the identification of thermal and compositional anomalies in the upper mantle. Earth and Planetary Science Letters, 2010, 289, 606-618.	1.8	68
18	3â€D multiobservable probabilistic inversion for the compositional and thermal structure of the lithosphere and upper mantle: III. Thermochemical tomography in the Westernâ€Central U.S Journal of Geophysical Research: Solid Earth, 2016, 121, 7337-7370.	1.4	67

#	Article	IF	CITATIONS
19	The lithospheric structure of the Western Carpathian–Pannonian Basin region based on the CELEBRATION 2000 seismic experiment and gravity modelling. Tectonophysics, 2009, 475, 454-469.	0.9	63
20	Thermochemical structure of the North China Craton from multi-observable probabilistic inversion: Extent and causes of cratonic lithosphere modification. Gondwana Research, 2016, 37, 252-265.	3.0	54
21	Lithospheric structure of the Gorringe Bank: Insights into its origin and tectonic evolution. Tectonics, 2010, 29, n/a-n/a.	1.3	53
22	Lithospheric structure in the Baikal–central Mongolia region from integrated geophysicalâ€petrological inversion of surfaceâ€wave data and topographic elevation. Geochemistry, Geophysics, Geosystems, 2012, 13, .	1.0	53
23	Geophysical-petrological modeling of the lithosphere beneath the Cantabrian Mountains and the North-Iberian margin: geodynamic implications. Lithos, 2015, 230, 46-68.	0.6	52
24	Tertiary tectonics of the sub-Andean region of the North Patagonian Andes, southern central Andes of Argentina (41–42°30′S). Journal of South American Earth Sciences, 2005, 20, 157-170.	0.6	49
25	The capacity of hydrous fluids to transport and fractionate incompatible elements and metals within the Earth's mantle. Geochemistry, Geophysics, Geosystems, 2014, 15, 2241-2253.	1.0	48
26	The deep lithospheric structure of the Namibian volcanic margin. Tectonophysics, 2010, 481, 68-81.	0.9	47
27	Sediment residence times constrained by uranium-series isotopes: A critical appraisal of the comminution approach. Geochimica Et Cosmochimica Acta, 2013, 103, 245-262.	1.6	46
28	Effects of compositional and rheological stratifications on smallâ€scale convection under the oceans: Implications for the thickness of oceanic lithosphere and seafloor flattening. Geophysical Research Letters, 2008, 35, .	1.5	45
29	The thermochemical structure of the lithosphere and upper mantle beneath south China: Results from multiobservable probabilistic inversion. Journal of Geophysical Research: Solid Earth, 2014, 119, 8417-8441.	1.4	45
30	Geophysicalâ€petrological model of the crust and upper mantle in the Indiaâ€Eurasia collision zone. Tectonics, 2016, 35, 1642-1669.	1.3	45
31	Arc–Continent Collision: The Making of an Orogen. Frontiers in Earth Sciences, 2011, , 477-493.	0.1	42
32	The effects of polybaric partial melting on density and seismic velocities of mantle restites. Lithos, 2012, 134-135, 289-303.	0.6	42
33	From the North-Iberian Margin to the Alboran Basin: A lithosphere geo-transect across the Iberian Plate. Tectonophysics, 2015, 663, 399-418.	0.9	34
34	The lithosphere–asthenosphere system beneath Ireland from integrated geophysical–petrological modeling II: 3D thermal and compositional structure. Lithos, 2014, 189, 49-64.	0.6	31
35	Decoupled crust-mantle accommodation of Africa-Eurasia convergence in the NW Moroccan margin. Journal of Geophysical Research, 2011, 116, .	3.3	30
36	How did the Dabie Orogen collapse? Insights from 3â€D magnetotelluric imaging of profile data. Journal of Geophysical Research: Solid Earth, 2016, 121, 5169-5185.	1.4	28

JUAN CARLOS AFONSO

#	Article	IF	CITATIONS
37	A poorly mixed mantle transition zone and its thermal state inferred from seismic waves. Nature Geoscience, 2021, 14, 949-955.	5.4	25
38	A wide-angle upper mantle reflector in SW Iberia: Some constraints on its nature. Physics of the Earth and Planetary Interiors, 2010, 181, 88-102.	0.7	23
39	Considerations for U-series dating of sediments: Insights from the Flinders Ranges, South Australia. Chemical Geology, 2013, 340, 40-48.	1.4	23
40	The lithosphere–asthenosphere system beneath Ireland from integrated geophysical–petrological modeling — I: Observations, 1D and 2D hypothesis testing and modeling. Lithos, 2014, 189, 28-48.	0.6	22
41	Elastic properties of three-phase composites: analytical model based on the modified shear-lag model and the method of cells. Composites Science and Technology, 2005, 65, 1264-1275.	3.8	20
42	Geochemical and geophysical constrains on the dynamic topography of the <scp>S</scp> outhern <scp>A</scp> frican <scp>P</scp> lateau. Geochemistry, Geophysics, Geosystems, 2017, 18, 3556-3575.	1.0	20
43	Lithosphere–asthenosphere interactions beneath northeast China and the origin of its intraplate volcanism. Geology, 2022, 50, 210-215.	2.0	19
44	Numerical modelling of multiphase multicomponent reactive transport in the Earth's interior. Geophysical Journal International, 2018, 212, 345-388.	1.0	18
45	The Deep Lithospheric Structure of the Junggar Terrane, NW China: Implications for Its Origin and Tectonic Evolution. Journal of Geophysical Research: Solid Earth, 2019, 124, 11615-11638.	1.4	18
46	Southwestern Africa on the burner: Pleistocene carbonatite volcanism linked to deep mantle upwelling in Angola. Geology, 2017, 45, 971-974.	2.0	17
47	The crustal structure of the <scp>A</scp> rizona <scp>T</scp> ransition <scp>Z</scp> one and southern <scp>C</scp> olorado <scp>P</scp> lateau from multiobservable probabilistic inversion. Geochemistry, Geophysics, Geosystems, 2016, 17, 4308-4332.	1.0	16
48	A reduced order approach for probabilistic inversions of 3-D magnetotelluric data I: general formulation. Geophysical Journal International, 2020, 223, 1837-1863.	1.0	16
49	LitMod2D_2.0: An Improved Integrated Geophysicalâ€Petrological Modeling Tool for the Physical Interpretation of Upper Mantle Anomalies. Geochemistry, Geophysics, Geosystems, 2020, 21, e2019GC008777.	1.0	14
50	Physical State and Structure of the Crust Beneath the Western entral United States From Multiobservable Probabilistic Inversion. Tectonics, 2018, 37, 3117-3147.	1.3	13
51	A Disequilibrium Reactive Transport Model for Mantle Magmatism. Journal of Petrology, 2021, 61, .	1.1	12
52	Thermochemical State of the Upper Mantle Beneath South China From Multiâ€Observable Probabilistic Inversion. Journal of Geophysical Research: Solid Earth, 2021, 126, e2020JB021114.	1.4	12
53	Thermochemical structure and evolution of cratonic lithosphere in central and southern Africa. Nature Geoscience, 2022, 15, 405-410.	5.4	12
54	Fast Stokes Flow Simulations for Geophysicalâ€Geodynamic Inverse Problems and Sensitivity Analyses Based On Reduced Order Modeling. Journal of Geophysical Research: Solid Earth, 2020, 125, e2019JB018314.	1.4	11

JUAN CARLOS AFONSO

#	Article	IF	CITATIONS
55	A Lagrangian–Eulerian finite element algorithm for advection–diffusion–reaction problems with phase change. Computer Methods in Applied Mechanics and Engineering, 2016, 300, 375-401.	3.4	10
56	Reworking of old continental lithosphere: Unradiogenic Os and decoupled Hf Nd isotopes in sub-arc mantle pyroxenites. Lithos, 2020, 354-355, 105346.	0.6	9
57	Improved geophysical image of the Carpathian-Pannonian Basin region. Acta Geodaetica Et Geophysica Hungarica, 2010, 45, 284-298.	0.4	8
58	New Constraints on the Thermal Conductivity of the Upper Mantle From Numerical Models of Radiation Transport. Geochemistry, Geophysics, Geosystems, 2019, 20, 2378-2394.	1.0	8
59	The deep thermochemical structure of the Dabie orogenic belt from multi-observable probabilistic inversion. Tectonophysics, 2020, 787, 228478.	0.9	8
60	Multiple Phase Changes in the Mantle Transition Zone Beneath Northeast Asia: Constraints From Teleseismic Reflected and Converted Body Waves. Journal of Geophysical Research: Solid Earth, 2018, 123, 6636-6657.	1.4	7
61	Melting Dynamics of Late Cretaceous Lamprophyres in Central Asia Suggest a Mechanism to Explain Many Continental Intraplate Basaltic Suite Magmatic Provinces. Journal of Geophysical Research: Solid Earth, 2021, 126, e2021JB021663.	1.4	7
62	An efficient and general approach for implementing thermodynamic phase equilibria information in geophysical and geodynamic studies. Geochemistry, Geophysics, Geosystems, 2015, 16, 3767-3777.	1.0	6
63	The hydrothermal power of oceanic lithosphere. Solid Earth, 2015, 6, 1131-1155.	1.2	6
64	Chemical Disequilibria, Lithospheric Thickness, and the Source of Ocean Island Basalts. Journal of Petrology, 2019, 60, 755-790.	1.1	5
65	A Reduced Order Approach for Probabilistic Inversions of 3D Magnetotelluric Data II: Joint Inversion of MT and Surfaceâ€Wave Data, Journal of Geophysical Research: Solid Earth, 2021, 126, .	1.4	5